Geologically Active – Williams et al. (eds)
© 2010 Taylor & Francis Group, London, ISBN 978-0-415-60034-7

Metamorphic rocks from Córdoba (Argentina) and the alkali-silica reaction

F. Locati & E. Baldo
CICTERRA-CONICET-UNC, Ciudad de Córdoba, Córdoba, Argentina

S. Marfil
CIC-INGEOSUR, Bahía Blanca, Buenos Aires, Argentina

O. Batic
CIC-LEMIT, La Plata, Buenos Aires, Argentina

ABSTRACT: The "Sierras Pampeanas de Córdoba" (Argentina) is an igneous-metamorphic complex affected by shear zones. The deformation varies from one sector to another producing microstructures that affect the internal order and the size of the crystals, generating sites susceptible to suffering the attack of alkaline solutions. This process, known as alkali-silica reaction (ASR), occurs between cryptocrystalline, strained and/or amorphous silica compounds and the alkalis in the concrete pore solution, and forms a gel that increases its volume producing cracks and concrete deterioration.

To evaluate the potential reactivity of rocks from the Córdoba region, the petrographic method (ASTM C 295), the accelerated mortar bar test method (ASTM C 1260) and the determination of dissolved silica (ASTM C 289) were carried out. The preliminary results allow determining a positive linear correlation ($R^2 = 0.86$) between the expansion in mortar bars and leached silica. These values grow with deformation intensity increment in quartz-bearing rocks.

1 INTRODUCTION

Most of the crushed rocks used in the construction industry in the central-east region of Argentina come from the eastern sector of the *Sierras Pampeanas de Córdoba*, Argentina (Fig. 1). They are mainly composed of gneisses, schists, migmatites, amphibolites, marbles and acidic, basic and ultrabasic igneous rocks (Baldo et al., 1996, Rapela et al., 1998). This igneous-metamorphic complex has been affected by ductile to brittle-ductile shear zones (Martino 2003) producing changes in the rock fabric due to intracrystalline deformation, recovery and recrystallisation processes (Passchier & Trouw 2005, Vernon 2004). At a microstructural level there is evidence of intracrystalline dislocations that cause undulatory extinction in quartz, development of lamellae and deformation bands and subgraining. Myrmekites (symplectic intergrowth of vermicular quartz and sodic plagioclase due to decomposition of potassic feldspar) are possibly also associated with deformation processes (Simpson & Wintsch 1989).

Dislocations cause a partial loss of continuity in the quartz crystal structure creating unstable sites that are susceptible to being attacked by the concrete pore solution (Jensen 1993, Wigum 1995a, Broekmans 2002). Quartz in myrmekites is also unstable (Rao & Sinha 1989).

Alkali ions can interact with the aggregates containing strained quartz and react with silica to produce alkali silicates that hydrate and increase in volume when water is present. Eventually, these compounds can incorporate calcium forming a more rigid and thicker grain boundary in the aggregate, which acts as a semi-permeable membrane that allows the ingress of alkali solutions and prevents the release of silicates that continue to be formed inside the aggregate (Ichikawa & Miura 2007).

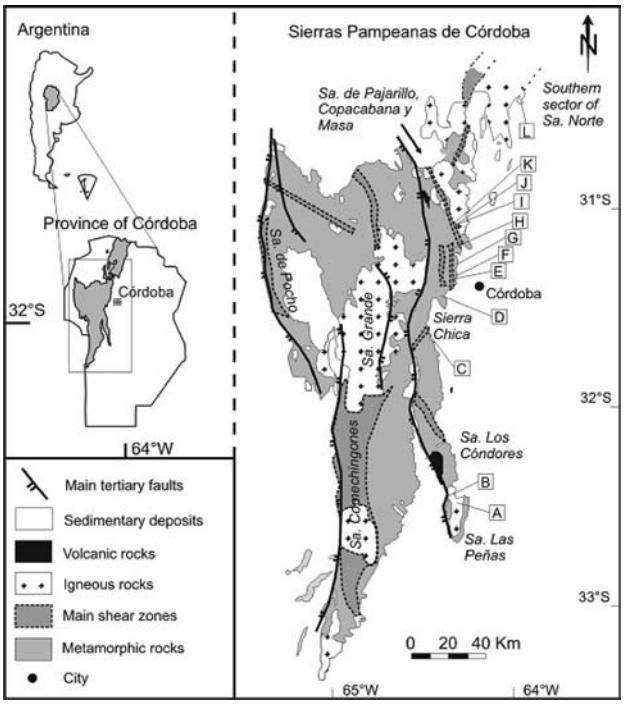

Figure 1. Geological map of the *Sierras Pampeanas de Córdoba*. Location of the samples studied (A to L). Modified from Martino (2003).

The process creates internal pressures that are so high that they exceed the resistance to internal stress in concrete causing the development of cracks that weaken the structure. This process is known as the alkali-silica reaction (ASR), and in rocks associated with strained quartz, a slow/late behaviour can be defined (Wigum 1995b, Swamy 1992, Ponce & Batic 2006) since deterioration is evidenced at longer times (10, 20 or 50 years) than when fast-reacting aggregates are used (1 to 5 years).

Alkali ions move into the aggregates through secondary permeability planes such as microcracks, rock foliation planes (Kerrick & Hooton 1992), grain boundaries or defective sites in the crystal structure of the minerals (Wigum 1995a).

To evaluate the potential alkali reactivity of the aggregates, a petrographic analysis was conducted first focusing on the identification of potentially reactive materials, and textures and microstructures associated with deformation processes (ASTM C 295). Then tests simulating the existing conditions in concrete were carried out to evaluate aggregate performance over short periods of time. The standard test methods more widely used are the accelerated mortar bar test method (ASTM C 1260) and the concrete prism test method (ASTM C 1293), although the latter is less used because of its long duration (1 year). The chemical test method (ASTM C 289) is used with some reservation owing to problems in identifying certain reactive aggregates.

The objective of this work is to compare dissolved silica values, as determined by the chemical test method, and mortar bar expansion (test methods) considering the species responsible for deleterious behaviour studied in previous work (Locati et al., 2009a, 2009b) and to characterise neoformation products in mortar bars.

2 MATERIALS AND METHODS

Samples of igneous and metamorphic rocks were taken from the eastern ridge of the *Sierras Pampeanas de Córdoba* covering regions of *Sierra de Las Peñas, Sierra Chica* and the southern

sector of *Sierra Norte*. The crushed rocks sampled come from quarries that are currently being exploited (G, H, L) and from potential outcrop areas (A, B, C, D, E, F, I, J, K).

The petrographic analysis of the different samples was performed as prescribed in the ASTM C 295 standard, focusing on the identification of potentially reactive mineralogies and on textures and microstructures favourable for ASR development (Locati et al. 2009a, 2009b).

Potential alkali reactivity was determined by the accelerated mortar bar test method (ASTM C 1260). It consists of moulding cement and sand bars ($25 \times 25 \times 285$ mm) with grain sizes, proportions, w/c ratio and mixing determined according to the aggregates to be evaluated. The bars are first cured in a fog room (24 hrs), then demoulded and immersed in water at 23°C in a sealed container and placed in a heater at 80°C (24 hrs). Once the length (initial) has been measured, they are immersed in a 1 N NaOH solution at 80°C for 14 days (a total of 16 test days) and the rest of the readings are taken. The standard prescribes that expansions below 0.10% at 16 days indicate aggregates of innocuous performance, and expansions above 0.20% a potentially deleterious behaviour. For expansions between 0.10% and 0.20% the aggregates are considered as marginal and it is recommended that supplementary information be gathered or further studies be made to be able to discriminate between innocuous and deleterious aggregates. Dissolved silica was determined as prescribed in the ASTM C 289 standard, which consists of crushing a fraction of the aggregate to be evaluated (between 300 μm and 150 μm in size) and placement of this fraction in a sealed container with a 1 N NaOH solution at 80°C for 24 hrs; the solution is then filtered and the dissolved silica in the liquid phase is determined.

Finally, studies with a stereomicroscope and by polarization microscopy on thin sections of the mortar bars were performed once the test time had elapsed, and neoformation products were characterised by SEM-EDS.

3 RESULTS

3.1 *Petrographic study*

A petrographic analysis was conducted, focusing mainly on potentially reactive mineralogies and the development of textures and microstructures related to deformation.

Sample A, "Metadiorite": Rock exhibiting granoblastic texture with polygonal crystal contacts, containing scarce anhedral quartz (2–5%), sizes ≤2 mm and with no evidence of intense deformation. Some grains show undulatory extinction or development of deformation bands. Subgraining is not very frequent.

Sample B, "Granetiferous gneiss": Rock with granolepidoblastic texture, containing abundant quartz (50%), of anhedral type and variable size (≤8 mm) where lower size quartz grains prevail (~1 mm). They are arranged in elongate bands and parallel to biotite, causing the main rock foliation. Deformation is evidenced by weak undulatory extinction, either in blocks or bands.

Sample C, "Serpentinite": Rock composed of globular masses of serpentine (85% to 90%), with a size ≤1 mm. Accessory minerals include calcite, opaque minerals and oxides. No quartz occurrence was observed.

Sample D, "Mylonitised gneiss": Rock with mylonitic foliation and abundant quartz (40%). It is arranged in elongate bands in the direction of rock foliation; they consist of small quartz grains with tortuous boundaries, which are sometimes diffuse and show undulatory extinction (≤1 mm). It exhibits patchy extinction, development of deformation bands and incipient subgrain formation.

Sample E, "Protomylonitised migmatite": Foliated rock with granolepidoblastic texture, containing anhedral quartz (20%) and bimodal grain-size distribution (~4 mm and ~25 μm). In recrystallised sectors it becomes euhedral. It shows abundant fluid inclusions and is arranged in elongate crystals with undulatory extinction and in blocks; there is deformation band development and subgrain formation (scarce). *Myrmekite formation is frequent.*

Sample F, "Heterogeneous migmatite": Slightly foliated rock, it has granoblastic texture with formation of light and dark bands, of similar composition to that of sample E. It is

different because it has a larger grain size (4–10 mm) and is of unimodal type. There is no evidence of shear deformation. The microstructures developed in quartz are similar to that of sample E, but here undulatory extinction prevails and there is greater development of myrmekites. Vermicular quartz that forms the myrmekitic texture is ~30 μm wide.

Sample G, "Amphibolite": It is a mixture of crushed rocks with fragments that range between 0.25 and 0.5 mm in size. The fragments come mainly from the crushed rocks of an amphibolite lens. They consist of monomineral particles and polymineral aggregates generically defined as amphibolitic and granitic. Quartz (< 5%) exhibits undulatory extinction, deformation bands and scarce subgraining (≤20 μm).

Sample H, "Mylonitised biotitic gneisses with and without garnet": Sample of crushed rocks between 0.25 and 0.5 mm in grain size. The fragments come mainly from crushed biotitic gneisses with and without garnet, both showing evidence of ductile deformation. They consist of monomineral particles and polymineral aggregates generically defined as gneissic. Quartz (~30%) exhibits undulatory extinction, development of deformation bands, subgrain formation (≤20 μm) and recrystallised grains.

Sample I, "Mylonitised granitoid": Rock having mylonitic texture with marked foliation (Fig. 2) and abundant quartz (40%–45%). It occurs in elongated and braided bands (~4 mm) with strong undulatory extinction. The development of deformation bands and subgrains that locally evolve into recrystallised grains (both ~20 μm in size) is common.

Sample J, "Deformed amphibolite": Rock with nematoblastic texture, containing scarce quartz (<5%), of anhedral type (≤100 μm) with undulatory extinction. It fills interstices or occurs in veins ~300 μm thick, although there are some ~20 μm thick.

Sample K, "Deformed orthogneiss": Rock with granolepidoblastic texture and gross foliation. It consists of quartz (35%) of size ≤2 mm, anhedral type and with net intergranular contacts. It generally shows undulatory extinction, and the development of lamellae and deformation bands is common. Subgrain formation is very incipient and is localised at some grain boundaries. The rock also shows the development of thin cataclastic bands associated with brittle deformation, where quartz crushing occurs, which is mainly associated with grain-grain contacts and the development of thin pseudotachylytes (maximum width 0.5 mm).

Sample L, "Mixture of granites": Mixture of crushed rocks between 0.25 and 0.5 mm in size, coming from crushed coarse-grained porphyritic granites and non-porphyritic facies of finer grain size. The fragments consist of monomineral particles as the grain size of the original rock was greater than the size of the crushed material. Quartz (32%) presents undulatory extinction although unstrained quartz prevails. There are some calcite aggregates that belong to alteration products of the original rock and aggregates from loessial material.

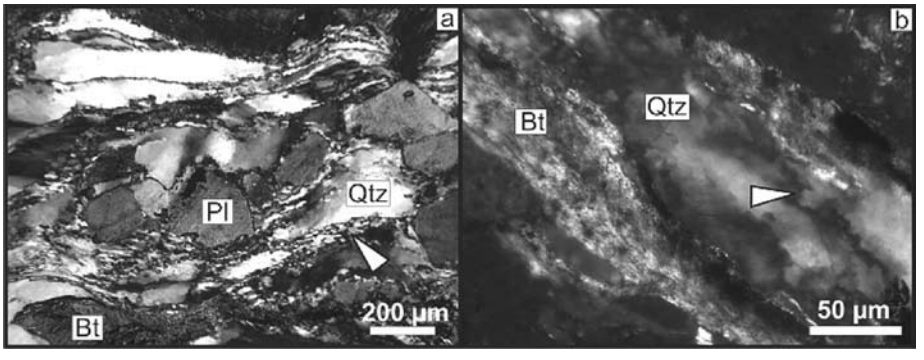

Figure 2. Micrographs of samples I (a) and H (b). a) Rock with mylonitic texture with marked foliation, development of quartz bands with undulatory extinction, subgraining and recrystallisation of boundaries (arrow). B) Aggregate of deformed biotitic gneiss showing quartz development with undulatory extinction and subgrain formation (arrow). Crossed nichols. Qtz: quartz, Bt: biotite, Pl: plagioclase.

Table 1. Dissolved silica (ASTM C 289) and length variation in mortar bars (ASTM C 1260).

Samples	Dissolved silica mg/l	Length variation (%) in mortar bars at different ages (days)				
		7	11	16	21	28
A	3.5	0.004	0.018	0.020	0.022	0.044
B	5.8	0.028	0.029	0.042	0.056	0.101
C	4.5	0.014	0.015	0.016	0.021	0.026
D	6.3	0.009	0.049	0.063	0.095	0.119
E	7.3	0.022	0.050	0.088	0.120	0.147
F	6.1	0.019	0.042	0.063	0.064	0.128
G	3.0	0.000	0.000	0.003	0.013	0.014
H	7.6	0.039	0.068	0.104	0.152	0.198
I	9.6	0.050	0.108	0.171	0.204	0.240
J	2.7	0.020	0.022	0.023	0.038	0.045
K	6.2	0.033	0.051	0.077	0.098	0.137
L	5.7	0.012	0.022	0.026	0.038	0.053

3.2 *Chemical test method and accelerated mortar bar test method*

The dissolved silica of the different samples was determined in accordance with the conditions set in the standard test method (ASTM C 289). The results are listed in Table 1, together with a summary of the expansion results of mortar bars at different ages (ASTM C 1260). In order to evaluate the potential alkali reactivity of the different samples likely to undergo a slow reaction, test time was extended to 28 days (Hooton & Rogers 1992, Falcone et al., 2008).

3.3 *Petrography of mortar bars*

In general, all mortar bars show no cracks, empty entrained air voids and good aggregate-paste bonding. Strong carbonation of the paste around voids and aggregates is sometimes observed.

Samples H and I are slightly carbonated but show development of perigranular, intergranular and sometimes intragranular microcracks that are lowly persistent and non-coalescent. The voids are partially or completely filled with both an isotropic material and a fibrous one with radial growth and low interference colour. The cracks are partially or completely filled with an amorphous and/or crystalline material with lamellar habit (Z) and low interference colour (Fig. 3). This material can occur inside particles and is generally related to strained quartz in the aggregate. It penetrates the aggregate through foliation planes, grain boundaries or through intracrystalline discontinuities that act as channels towards the interior of the aggregate.

3.4 *SEM-EDS*

SEM images taken of the mortar bar made with aggregates I allow characterizing the material that fills entrained air voids and perigranular cracks (Z) as a mineral with lamellar or platy habit arranged as a rosette (Fig. 4a). According to the EDS diagram (Fig. 4b) it is a sodium silicate containing some calcium. There are also some crystals with fibrous habit that cross-cut the rosettes and are similar in composition although with a higher calcium content (Fig. 4c).

4 DISCUSSION

The potential alkali reactivity of basaltic rocks was evaluated in previous work (Marfil et al., 1998) and good correlation was observed between dissolved silica and mortar bar expansion.

Dissolved silica values were compared at a 24-hour test time and mortar bar expansion at 28 days (Fig. 5). Good correlation was determined between both values by the calculation

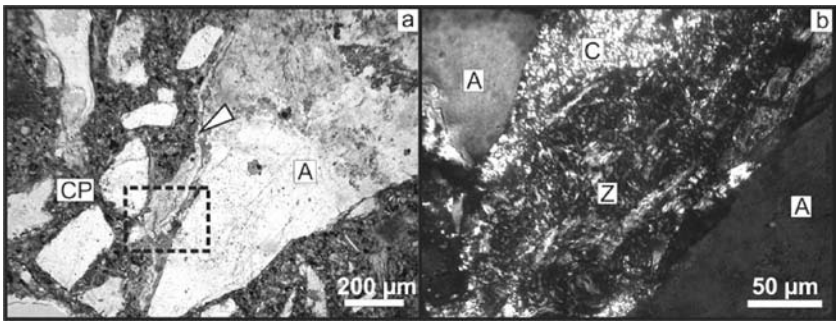

Figure 3. Micrographs of the mortar made with aggregates I. a) Development of a perigranular crack at the paste-aggregate interface (arrow) that increases in thickness (black dotted-line rectangle). Parallel nichols. b) Detail of the same crack in the zone where it becomes thicker. Crystallisation of a material with fibrous to lamellar habit and low interference colour that fills the crack is observed (Z), as well as paste carbonation (C) at the paste-aggregate interface. Crossed nichols. CP: cement paste, A: aggregate.

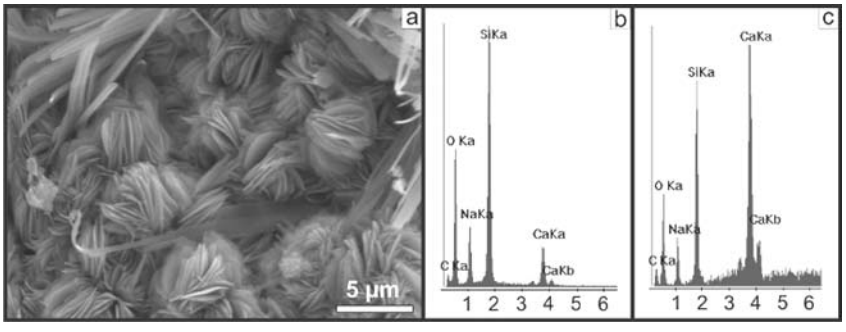

Figure 4. SEM image and EDS diagrams of neoformation materials in the mortar bar made with aggregates I. a) Development of rosette-like crystals with a fibrous habit in an entrained air void. b) Composition of rosette-like crystals. c) Composition of crystals with fibrous habit.

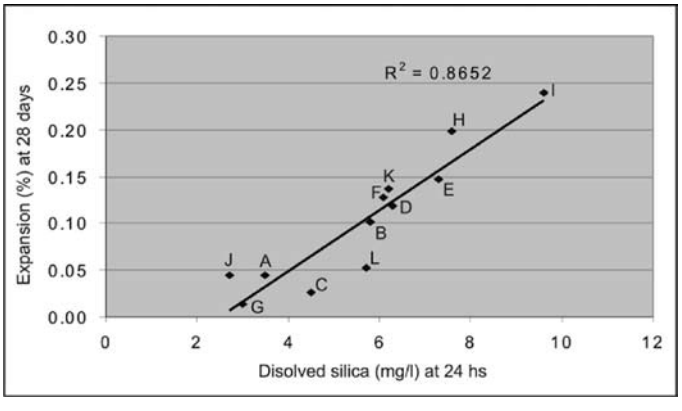

Figure 5. Comparison between dissolved silica values of the samples at 24 hrs and mortar bar expansion at 28 days.

of the correlation coefficient ($R^2 = 0.8652$). However, it is worth noting that in the study conducted by Marfil et al. (1998) fast-reacting rocks were evaluated, whereas in this work slow-reacting rocks were studied. In order to achieve a better fit of the straight line and determine more reliable ranges, a larger number of samples shall be studied. Dissolved silica values

allow inferring the potential performance of the aggregates under high-alkali conditions. However, for a better evaluation of the potential alkali reactivity it is important to consider other rock characteristics, such as quartz content, the development of foliation structures, microstructures associated with strained quartz, and grain and subgrain size. For example, samples G and J correspond to amphibolites with a very low quartz content (<5%) and they both had similar dissolved silica values (~3 mg/l). However, sample J shows greater expansion possibly due to the development of more marked foliation structures because of mylonitisation and the development of quartz veins that possibly are of hydrothermal origin.

Sample A corresponds to metadiorite and sample L to a mixture of granites, both being slightly deformed igneous rocks. They both gave similar expansion percentages (~0.05%). However, sample L contains approximately 30% more quartz and thus showed a higher value of dissolved silica. There are two behaviours that are worth noting. The first one is that at 28 days of test time some samples continue expanding without being stabilised. The other is that some samples release much silica despite their low expansion percentage. This could be indicating that the accelerated mortar bar test method underestimates the expansion percentage of slow-reacting samples and that new limits or longer test times are required to evaluate this type of aggregate. Nevertheless, it should be taken into account that the silica release test is very aggressive as the sample is crushed to very small grain sizes (between 300 μm and 150 μm) and hence the specific surface of attack is much greater than in mortar bar aggregates.

In this regard, and observing the graph of Figure 5, three categories could tentatively be defined. A first group with expansions between 0.0 and 0.05% and silica release values between 2 and 6 mg/l; a second group with expansions between 0.10 and 0.15% and silica values between 6 and 8 mg/l; and a third group with expansions between 0.20 and 0.25% and silica values between 8 and 10 mg/l. The latter was the most affected, showing microcracking of the paste and the paste-aggregate interface.

As was concluded in the first phase of this work (Locati et al., 2009b), the reactivity of these slow-reacting rocks depends not only on their petrographic classification but also on the concurrence of factors that make them more susceptible to reacting and causing the ASR in concrete (provided humidity is high and alkalis are available).

In general, the higher the rock quartz content, the more marked its foliation, the larger the number of microstructures associated with strained quartz are and the closer the grain size is to a dozen microns, the higher the aggregate potential reactivity results (Locati et al., 2009b).

In regard to neoformation products, it is important to point out that the short duration of the accelerated mortar bar test method usually does not allow crystallisation of ASR products, although it is useful for characterizing the degree of cracking in the mortar and evaluating the paste-aggregate interface. However, the mortar bar where aggregates I were used showed evidence of crystallisation of a mineral with lamellar or platy habit and low interference colour in the perigranular cracks associated with strained quartz aggregates. This mineral was identified as sodium silicate (possibly hydrated) containing some calcium.

The minerals with fibrous habit that cross-cut the rosettes possibly correspond to hydrated calcium silicates from cement hydration. Owing to the small thickness of these needles, the composition shown in EDS diagrams is possibly an average due to interference with the underlying lamellar material.

5 CONCLUSIONS

In this work a good correlation ($R^2 = 0.8652$) was observed between mortar bar expansion and the silica released from the rocks tested. In addition, the higher the rock quartz content, the more marked its foliation, the larger the number or microstructures associated with strained quartz are and the closer the grain size is to some dozen microns, the greater aggregate expansion results. Although each test has a variability range, when the potential reactivity of the aggregates is evaluated, plotting graphs or patterns that link different results may prove more useful than using a single test method.

Of the rocks analysed, both samples H and I behaved as potentially reactive with respect to the ASR (ASTM C 1260). Sample I gave the highest expansion (0.24% at 28 days) and alkali release (9.6 mg/l) values. This behaviour is the result of the intense deformation undergone by the rock and hence a combination of compositional, textural and microstructural characteristics that turned it more susceptible to alkali attack in the concrete pore solution.

The material identified in the mortar bar made with aggregate I is sodium silicate (possibly hydrated) with a lower calcium content, with lamellar or platy habit, arranged as a rosette, which is crystallised in perigranular cracks and entrained air voids, and is considered to be a crystalline product of the ASR.

REFERENCES

ASTM C 289. 1995. Standard test method for potential alkali reactivity of aggregates. (Chemical Method). *Annual Book of ASTM Standards, 4.02. ASTM*. Philadelphia, USA.

ASTM C 295. 1995. Standard test method for potential alkali reactivity of aggregates. (Petrographic Method). *Annual Book of ASTM Standards, 4.02. ASTM*. Philadelphia, USA.

ASTM C 1260. 1994. Standard test method for potential alkali reactivity of aggregates (Accelerated Method). *Annual Book of ASTM Standards, 4.02. ASTM*. Philadelphia, USA.

ASTM C 1293. 2001. Standard test method for concrete aggregates by determination of length change of concrete due to alkali-silica reaction. *Annual Book of ASTM Standards, 04.02. ASTM*. PA., USA.

Baldo, E.G., Casquet, C. & Galindo, C. 1996. El metamorfismo de la Sierra Chica de Córdoba (Sierras Pampeanas). Argentina. *Geogaceta* 19: 51–54.

Broekmans, M.A.T.M. 2002. *The alkali-silica reaction: mineralogical and geochemical aspects of some Dutch concretes and Norwegian mylonites*. PhD Thesis, Utrecht University, 144 pp.

Falcone, D., Sota, J. & Batic, O. 2008. Discusión sobre métodos para evaluar agregados potencialmente reactivos. *III Cong. Internacional de la AATH - 17ª Reunión Técnica*, 329–336, Córdoba - Argentina.

Hooton, R.D. & Rogers, C.A. 1992. Development of the NBRI rapid mortar bar test leading to its use in North America. *9th ICAAR* (1): 461–467, London.

Ichikawa, T. & Miura, M. 2007. Modified model of alkali-silica reaction. *CCR*. 32: 1291–1297.

Jensen, V. 1993. *Alkali aggregate reaction in southern Norway*. PhD Thesis, Univ. of Trondheim, 262 pp.

Kerrick, D.M. & Hooton, R.D. 1992. ASR of concrete aggregate quarried from a fault zone: results and petrographic interpretation of accelerated mortar bar test. *Cem. Concr. Res*. 22: 949–960.

Locati, F., Marfil, S., Batic, O. & Baldo, E. 2009a. Rocas de las sierras de Córdoba como agregados para hormigón. Comportamiento frente a la Reacción Álcali-Sílice (RAS). *9° Simposio de Geología Aplicada a la Ingeniería y al Ambiente*, Mar del Plata, Buenos Aires, CD, 2 pp. (Abstract)

Locati, F., Marfil, S., Batic, O. & Baldo, E. 2009b. Rocas de las sierras de Córdoba como agregados para hormigón. Comportamiento frente a la RAS. *Revista ASAGAI – Argentina. (In press)*.

Marfil, S., Maiza, P., Bengochea, A., Sota, J. & Batic, O. 1998. Relationships between SiO_2, Al_2O_3, Fe_2O_3, CaO, K_2O, and expansion in the determination of the alkali reactivity of basaltic rocks. *Cem. Concr. Res*. 28 (2) 189–196.

Martino, R.D. 2003. Las fajas de deformación dúctil de las Sierras Pampeanas de Córdoba: Una reseña general. *Revista de la Asociación Geológica Argentina* 58 (4): 549–571.

Ponce, J.M. & Batic, O.R. 2006. Different manifestations of the alkali-silica reaction in concrete according to the reaction kinetics of the reactive aggregate. *Cem. Conc. Res*. 36: 1148–1156.

Passchier, C.W. & Trouw, R.A.J. 2005. *Microtectonics (2nd Ed.)*, Berlin: Springer-Verlag.

Rao, L.H. & Sinha, S.K. 1989. Textural and microstructural features of alkali reactive Granitic rocks. In K. Okada, S. Nishibayashi & M. Kawamura (eds.), *8th ICAAR*, Kyoto: 495–499.

Rapela, C., Pankhurst, R., Casquet, C., Baldo, E., Saavedra, J., Galindo, C. & Fanning, C. 1998. The Pampean Orogeny of the southern proto-Andes: Cambrian continental collision in the Sierras de Córdoba. In: *The Proto-Andean Margin of Gondwana*, *Geol. Soc. London Spec. Publ*. 142: 181–217.

Simpson, C. & Wintsch, R. 1989. Evidence for deformation-induced K-feldspar replacement by myrmekite. *J. Metam. Geol*. 7: 261–275.

Swamy, R.N. (ed.) 1992. *The Alkali–Silica Reaction in Concrete*. Glasgow and London: Blackie and New York: Van Nostrand-Reinhold.

Vernon, R.H. 2004. *A Practical Guide to Rock Microstructure*. United Kingdom: Cambridge Univ. Press.

Wigum, B.J. 1995a. *Alkali–aggregate reactions in concrete: properties, classification and testing of Norwegian cataclastic rocks*. Doctor Ingeniør thesis, University of Trondheim, 227 pp.

Wigum, B.J. 1995b. Examination of microstructural features of Norwegian cataclastic rocks and their use for predicting alkali-reactivity in concrete. *Eng. Geol*. 40: 195–214.